



Study on TBM jamming hazard in Opalinus clay

Conference Paper**Author(s):**

Nordas, Alexandros ; Natale, Matteo; Anagnostou, Georgios ; Cantieni, Linard

Publication date:

2023-04-12

Permanent link:

<https://doi.org/10.3929/ethz-b-000614351>

Rights / license:

Creative Commons Attribution-NonCommercial-NoDerivatives 4.0 International

Originally published in:

<https://doi.org/10.1201/9781003348030-258>

Study into the TBM jamming hazard in Opalinus clay

A.N. Nordas, M. Natale & G. Anagnostou
ETH Zurich, Zurich, Switzerland

L. Cantieni
National Cooperative for the Disposal of Radioactive Waste (Nagra), Wettingen, Switzerland

ABSTRACT: The National Cooperative for the Disposal of Radioactive Waste (Nagra) in Switzerland has designated Opalinus clay as a host rock for a deep geological repository. The drifts for high-level waste storage (\varnothing 3.5 m) are to be constructed with a shielded tunnel boring machine (TBM) at depths where squeezing conditions may occur and the ground is fully saturated. This paper studies the TBM shield jamming hazard during excavation or long TBM stand-stills by means of 3D, transient, coupled hydraulic-mechanical Finite Element computations. An anisotropic linearly elastic and perfectly plastic constitutive model with a Mohr Coulomb yield condition is adopted for the Opalinus clay. Of practical interest is the influence of anisotropy and ground desaturation on the time-dependent ground deformations after excavation. The study concludes that shield jamming is not critical. The results offer practical guidance for the identification of critical design aspects for underground systems in pronouncedly anisotropic ground.

1 INTRODUCTION

In Switzerland, high-level waste (HLW) will be stored in cylindrical drifts with external and internal diameters of 3.5 m and 2.8 m, respectively, embedded in Opalinus clay (Figure 1). In the repository siting regions under consideration in the last stage of the site selection process, the Opalinus clay layer is *ca.* 100 m thick, fully saturated, and interspersed between permeable layers of calcareous and argillaceous marls at depths ranging from 600 to 900 m. The drifts are to be constructed with a shielded tunnel boring machine (TBM) and supported by a segmental concrete lining. Squeezing conditions, characterized by the development of significant rock pressure upon the shield and the lining, may be encountered at the depths under consideration. Hence, the most critical hazards are over-stressing of the segmental lining and jamming of the TBM shield, which occurs when the installed thrust force in the TBM is insufficient to overcome the frictional forces developing upon contact of the shield with the ground (Ramoni & Anagnostou 2010).

This paper presents a detailed numerical assessment of the shield jamming hazard for the deepest planned repository location with 900 m overburden. By virtue of the presented investigations, the paper aims to improve the understanding of the influence that material anisotropy and ground desaturation have on the excess pore pressure dissipation and ground consolidation. In this sense, it also offers general guidance for considering these aspects in the design of deep geological repositories and, more generally, underground systems in low-permeability anisotropic rock.

The paper starts with a discussion on the key geological features and the anisotropic mechanical behaviour of Opalinus clay in Section 2. Section 3 discusses the conditions during excavation that lead to the development of negative pore pressures and potential ground desaturation. Section 4 performs a preliminary assessment of the convergences, while Section 5 describes the 3D computational model employed for the detailed assessment of shield jamming. Section 6 examines the development and dissipation of excess pore pressures in the vicinity of the tunnel, with specific focus on the influence of ground desaturation and anisotropy. Finally, Section 7 demonstrates the influence of these effects on shield jamming and evaluates the necessary TBM overcut.

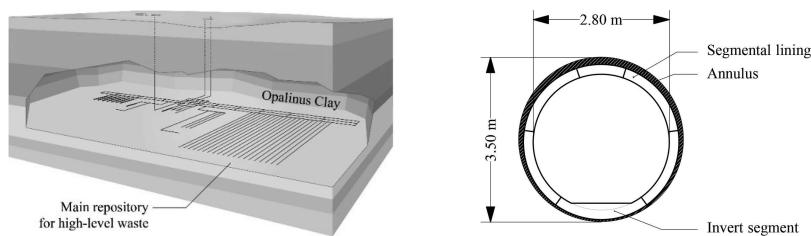


Figure 1. Schematic layout of the underground facility (left); cross section of a HLW drift (right).

2 DESCRIPTION OF OPALINUS CLAY

Opalinus Clay consists mostly of grey to black, silty to sandy claystones. It was formed in a shallow epicontinental sea during the early Middle Jurassic period and upon deposition experienced a complex evolution (Mazurek et al. 2006). The maximum burial depth of *ca.* 1500-2000 m developed in the Miocene, followed by uplift to present depths of *ca.* 400-1000 m in the repository sites. Opalinus Clay exhibits similar properties to the Callovo-Oxfordian claystone, the designated host rock for a radioactive waste repository in France (e.g., Armand et al. 2017), as well as many caprocks (or top seals) for hydrocarbon reservoirs. Compared to “classic” clays, such as London Clay, it is characterised by much lower porosity and higher strength.

The strength and stiffness properties of Opalinus clay have been investigated by means of consolidated drained and undrained triaxial compression tests on specimens obtained from deep boreholes in the repository sites under consideration. Due to the expectation that Opalinus clay will have a pronouncedly anisotropic behaviour, the tests were performed for various bedding orientations (Crisci *et al.* 2021, 2022). Figure 2 shows the typical experimental behaviour of samples with the same initial confining pressure in the various test types. The results indicate: (i) slightly nonlinear behaviour right from the start of loading; (ii) stiffness anisotropy (maximum stiffness in P-tests parallel to the bedding and minimum stiffness in S-tests orthogonal to the bedding); (iii) strength anisotropy (lower strength for failure along the bedding in Z-tests compared to failure through the matrix in S- and P-tests); and (iv) practically brittle strain softening in the rock matrix and bedding. Additionally, (v), moderate stiffness dependency on the initial confining pressure was observed (not visible in Figure 2).

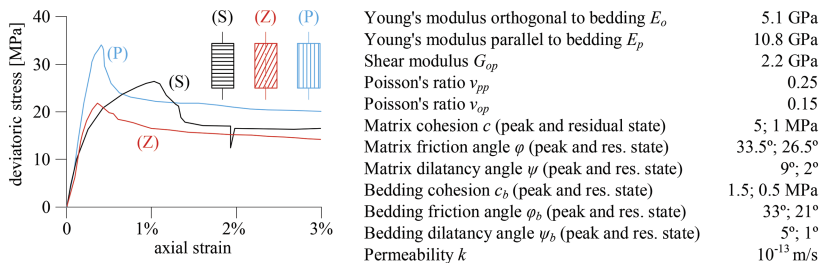


Figure 2. Typical experimental behaviour of Opalinus clay in triaxial compression tests (after Crisci *et al.* 2021, 2022, tests C1_TRU1_1, C13T_BUL1-1 and C9_BOZ2_1) and material constants at 900 m depth (after Brauchart *et al.* 2021).

To simulate the behaviour of Opalinus clay, an extension of the common linear elastic and perfectly plastic constitutive model with a Mohr-Coulomb yield criterion and a non-associated plastic flow rule is adopted, which additionally considers the aforementioned stiffness and strength anisotropy. The model behaviour is fully defined via 11 constants, as listed in the table inside Figure 2. While the model can readily reproduce anisotropy with a single set of material constants, it is incapable of capturing pre-peak nonlinearity, softening, and stiffness dependency on the initial confining pressure. These limitations are circumvented by considering: (a)

nonlinearity via the secant stiffness modulus at 50% of peak strength, which is accurate for tunnelling problems under squeezing conditions (Vrakas et al. 2018); (b) softening via two borderline cases for the peak and residual states; and, (c), stiffness dependency on initial confining pressure by considering the values of the Young's moduli E_o and E_p that hold at the expected *in situ* stress (cf. Vrakas et al. 2018). The typical material constants for Opalinus clay as determined from the experimental data are given in Figure 2. These values correspond to a 900 m overburden and will be used later for the numerical computations. (The constants after Figure 2 are slightly different than the ones adopted in the companion paper by Morosoli *et al.*, 2023, because they are based upon an earlier preliminary calibration.)

3 CONDITIONS DURING EXCAVATION

Excavation causes an unloading of the tunnel boundary. Below a certain value of the support pressure, the ground yields plastically in a zone around the tunnel (so-called “plastic zone”). In the absence of water, the unloading would result in volumetric increase inside the plastic zone (due to plastic dilatancy and stress reduction). In low-permeability, water-bearing ground, such as Opalinus clay ($k=10^{-13}$ m/s), practically undrained conditions prevail during excavation since seepage flow takes place extremely slowly and the extent of the consolidation is negligible. Therefore, the water content remains constant, which is equivalent to zero volumetric deformations (assuming incompressible ground constituents, *i.e.*, solid grains and pore water, which is realistic for weak rocks). Due to this volumetric constraint, the tunnel unloading is accompanied by a decrease in pore pressures in the plastic zone. Depending on *in situ* stress and hydrostatic pressure, support pressure and ground parameters, the pore pressure may even become negative (“suction”). This is thoroughly possible in the present case, considering the high *in situ* stresses.

The suction has a stabilising effect, since it increases the effective stresses and hence the shear resistance of the ground. However, it may result in air entry into (and thus desaturation of) the ground. Although claystones may remain saturated even under high negative pore pressures (Chenevert 1969), it is thoroughly possible that cracks develop and open around the tunnel during excavation, thus inducing desaturation. The latter would invalidate the zero volumetric strain assumption and lead to partial or complete loss of the stabilising effect of negative pore pressures and, in turn, to bigger plastic deformations and convergences.

Considering the possibility of (unfavourable) ground desaturation, it is worth conducting an in-depth investigation into the mechanism underlying excess pore pressure generation. This is done later, in Section 6, paying particular attention to the effect of stiffness anisotropy.

The development of excess pore pressures and the drainage action of the tunnel trigger seepage flow in the surrounding ground. This enables the progressive dissipation of the excess pore pressures and results in ground consolidation. Due to the extremely low permeability of Opalinus clay, this process is pronouncedly time dependent, playing a role in the long-term behaviour of the tunnels, but having only subordinate importance for the processes in the vicinity of the advancing tunnel face.

4 PRELIMINARY ASSESSMENT OF THE SHORT-TERM CONVERGENCES

A rough estimate of the convergences that occur during excavation in the vicinity of the advancing tunnel face can be obtained using closed-form solutions for the ground response curve (GRC) under undrained conditions in elastoplastic ground, considering either a perfectly plastic ground (Anagnostou 2009) or a brittle-plastic ground (Nordas & Anagnostou 2021). The assumption of brittle-plastic behaviour appears reasonable in view of the experimental results (see diagram in Figure 2), which indicate a rather sudden drop in strength after some deformation, while the perfectly plastic model (in combination with the residual or with the peak strength parameters) serves to bound the possible range of ground response. A GRC describes the relationship between the radial displacement u_a of the tunnel boundary and the support pressure σ_a applied thereat, assuming plane strain conditions. The common assumptions of rotational symmetry are embedded in the solutions, *i.e.* a deep, cylindrical and uniformly supported tunnel crossing

homogeneous and isotropic rock, with homogeneous and isotropic initial stress and pore pressure fields. Additionally, the ground is assumed to remain fully saturated under negative pore pressures, and a zero dilatancy angle ($\psi = 0^\circ$) is considered. This is equivalent to zero plastic volumetric deformations, and is in fact a conservative assumption, since it results in lower suction and thus less stabilisation of the ground, and in turn larger displacements.

Figure 3 shows the GRCs, for a 3.5 m diameter tunnel (Figure 1), the minimum Young's modulus ($E_o = 5.1$ GPa), $\nu = 0.15$ and the strength parameters of either the rock matrix (l.h.s. diagram) or the bedding plane (r.h.s. diagram). It is remarkable that the predictions of the brittle plastic material model are very close to those of a perfectly plastic model with residual parameters.

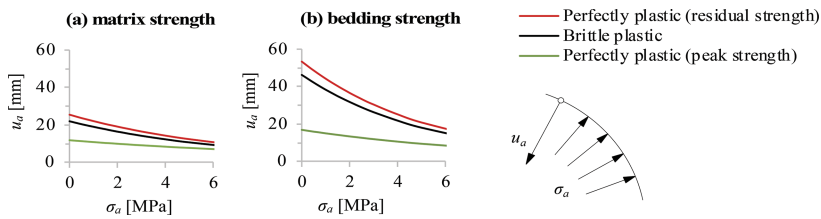


Figure 3. Ground response curves.

The results indicate a maximum radial ground displacement of 55 mm. Considering that about 30 to 50% of the displacements occur ahead of the tunnel face, a moderate TBM cutter-head overcut of about 30 to 40 mm is required to completely avoid contact between the ground and the shield.

Notwithstanding the favourable results of these preliminary investigations, a more accurate assessment of the shield jamming hazard is needed to consider additional aspects that plane strain solutions neglect: (i) the potential partial drainage and consolidation which may occur during construction, particularly during longer excavation standstills, resulting in greater convergences; (ii) the expected anisotropy of the *in situ* stress field (Nagra 2016); (iii) the effect of material anisotropy on the pore pressure, stress and displacement distributions around the tunnel, which can locally increase convergences in parts of the tunnel cross-section; and (iv) the unfavourable influence of potential desaturation of the Opalinus clay on convergences (*cf.* Section 3).

A detailed spatial simulation of the mechanised excavation is carried out with a 3D coupled hydraulic-mechanical Finite Element (FE) model, taking all the above into consideration. The model is presented in Section 5 and the results of the spatial simulations in Sections 6 and 7.

5 COMPUTATIONAL MODEL

A 3D coupled hydraulic-mechanical FE model has been developed in Abaqus[®] (Dassault Systèmes 2019) to simulate step-by-step drift excavation and lining installation sequences (Figure 4). Due to the uncertainty about the effect of high negative pore pressures on ground saturation, two borderline cases are considered: (i) the ground remains 100% saturated; and (ii) the ground fully desaturates and atmospheric pressure ($p_w = 0$ MPa) prevails in regions where negative pore pressures would otherwise develop (so-called “suction cut-off”). The latter is considered via the specification of a sorption curve that prescribes 0 pore pressure for saturation levels below 100%. For the sake of simplicity, a desaturation-induced reduction in permeability is not considered. This effect may influence the time-development of deformations (and thus the duration of the consolidation process) but is irrelevant for the instantaneous response during excavation.

On account of the high permeability contrast between Opalinus clay and the adjacent formation, the *in situ*, hydrostatic, pore pressure ($p_{w0} = 9$ MPa) is prescribed at their interface, 50 m above and below the tunnel axis (Figure 4). The far-field boundaries of Opalinus clay are taken as impervious. At the tunnel boundary two different hydraulic boundary conditions are considered, depending on the adopted assumption for desaturation: (i) when the ground

remains fully saturated, thus sustaining negative pore pressures, a mixed condition is considered that enables seepage flow solely from the rock to the tunnel but not vice versa; and, (ii), when the ground fully desaturates, atmospheric pressure ($p_w = 0$) is considered. The *in situ* stress state is taken anisotropic with earth pressure coefficient $K_z = 1.3$ in the longitudinal direction (Nagra 2016) and vertical stress $\sigma_0 = 22.5$ MPa at 900 m depth.

The anisotropic linearly elastic and perfectly plastic constitutive model of Section 2 is adopted for Opalinus clay, taking account of the horizontal bedding and the residual strength parameters (after Figure 2). The latter is reasonably conservative (Section 4, Figure 3). The far-field rock and the concrete lining are modelled as linearly elastic materials with $E = 5$ GPa and $E = 30$ GPa, respectively.

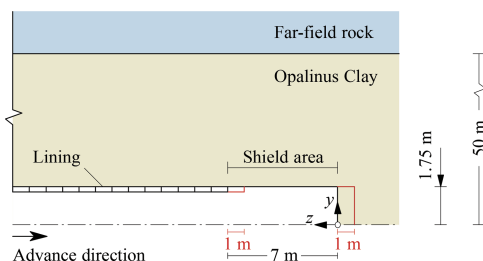


Figure 4. Part of the computational domain (vertical symmetry plane; not in scale).

The numerical simulation considers the excavation of a 30 m long tunnel stretch, assuming a gross advance rate of 5 m/day. At each excavation step, 1 m of ground is removed at the advancing face and 1 m of segmental lining is installed immediately behind the 7 m long TBM shield. Rather than modelling the shield-ground contact problem, the assumption is made that the overcut of the TBM cutter head is sufficient to avoid any contact between them; the shield is thus not a component of the statical system, but instead an unsupported span equal to the shield length is considered. These computations enable the minimum required overcut to be determined from the maximum convergence (*i.e.*, maximum ground displacement relative to the tunnel face) of the ground around the shield.

Two design situations are taken into account: (i) the conditions during ongoing mechanised excavation and support installation; and (ii) the conditions after a 1-year long TBM standstill. In both cases the full length of 30 m is considered excavated. The standstill duration of 1 year is selected as an adverse scenario.

6 DEVELOPMENT AND DISSIPATION OF EXCESS PORE PRESSURE

As discussed in Section 3, the ground consolidation that is associated with the dissipation of the excavation-induced excess pore pressures is a pronouncedly time-dependent process. This section examines in detail the effects of ground desaturation and material anisotropy on this process.

Figure 5 shows contour plots of the pore pressure field in the vertical symmetry plane during TBM advance, after a 1-year long TBM standstill and at steady state (1000 years after completion of excavation and lining installation).

If the ground can sustain suction without desaturation, negative excess pore pressures develop around the tunnel over its full length and ahead of the face (red zone in Figure 5a). After 1 year of standstill, the negative pressures have completely dissipated (zero pressure) above the stiff lining, which prevents additional deformations, but persist locally over the unsupported ground above the shield, which is free to deform (Figure 5b). The change in the excess pore pressure field during the standstill is remarkable and indicates that considerable consolidation takes place within 1 year. At steady state (Figure 5e), excess pressures have completely dissipated; the pore pressure increases gradually from atmospheric (prevailing everywhere at the tunnel boundary) to the *in situ* hydrostatic pressure (prevailing at the interface of the Opalinus clay with the adjacent rock; Figure 4).

In the case of desaturation, atmospheric pressure readily prevails over the entire tunnel boundary during TBM advance, roughly in the area where negative pressures would otherwise

develop (compare Figure 5a, c). Therefore, the pore pressure field does not change much during the 1 year of standstill, either in the supported ground around the lining or in the unsupported ground around the shield (Figure 5d); changes are observed only ahead of the tunnel face. Consequently, the extent of ground consolidation during 1 year is negligible. At steady state, the pore pressure distribution is identical to the case without desaturation (Figure 5e).

To assess the additional influence of anisotropy, Figure 6 shows the pore pressure field distributions in the radial directions beside the sidewalls and above the crown of the tunnel at the section in the middle of the shield (3.5 m behind the tunnel face), during advance (red lines), after a 1-year-long standstill (blue lines) and at steady-state conditions (black lines).

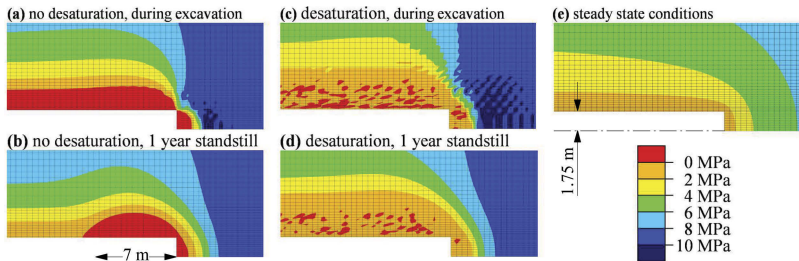


Figure 5. Contour plots of pore pressure field in the vertical symmetry plane.

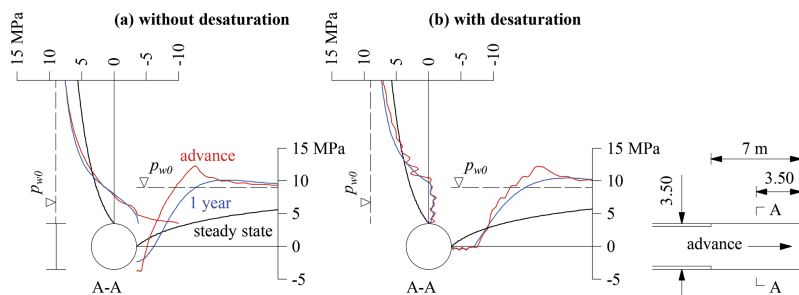


Figure 6. Radial pore pressure distributions.

In the case without desaturation (Figure 6a), the suction developing during TBM advance is higher at the crown than at the sidewalls due to stiffness anisotropy; in an isotropic material the negative pore pressure is uniform over the tunnel boundary (*cf.* Anagnostou 2009). A qualitative explanation is given hereafter: at the crown, cavity unloading results in an expansion in the lower-stiffness direction (*i.e.*, normal to the bedding) and a contraction in the higher-stiffness direction (*i.e.* parallel to the bedding). The overall effect is thus expansion or, under undrained conditions, development of negative rather than positive excess pore pressures. The opposite happens beside the sidewalls; the rock experiences expansion parallel to the bedding (in the higher-stiffness direction) and contraction normal to the bedding (in the lower-stiffness direction). The overall effect is thus contraction rather than expansion and, under undrained conditions, development of positive rather than negative excess pore pressures. This is why the highest suctions develop above the crown.

Anisotropy also affects the pore pressures far away from the tunnel; they are higher than the *in-situ* pore pressure p_{w0} above the crown, but lower than p_{w0} beside the tunnel. After 1 year of standstill, negative pore pressures have partially dissipated, mainly in the vicinity of the tunnel boundary, however the influence of anisotropy discussed above is still apparent. The variation of the distributions within 1 year indicates that ground consolidation takes place, as confirmed by Figures 5a, b. At steady state, an identical pore pressure distribution is obtained both at the crown and at the sidewalls (and over the entire cross-section), and the

influence of anisotropy of the mechanical behaviour vanishes. (Opalinus clay also exhibits a permeability anisotropy. The latter is not taken into account here, but would also influence the steady-state pore pressure field.)

In the case with desaturation, the influence of anisotropy on the pore pressures prevailing around the desaturated zone is still visible (Figure 6b). The desaturated zone is larger than the region of negative pressures in the case without desaturation (compare Figure 6a, b). This is because the evolution of the pore pressure field during unloading is different in the two cases (in the case with desaturation the water content changes within the desaturated zone). After 1 year of standstill the distributions change very little, mainly in the region of positive pressures away from the tunnel (where the influence of anisotropy is still visible), and consequently the extent of consolidation is negligible. The final distributions at steady state conditions are identical at the crown and sidewalls, and identical to the case without desaturation (Figure 6a, b).

It should be noted that the pore pressure oscillations within the desaturated regions in Figure 6b (and the red spots in Figure 5c, d) are of a purely numerical nature and are attributed to the suction cut-off implementation in Abaqus[®], which allows for small negative pore pressures to ensure numerical stability. The maximum allowable magnitude of negative pressures is about 0.5 MPa, which is negligible compared to the magnitude of negative pressures without desaturation (6-10 MPa; *cf.* Figure 6a) and to the magnitude of positive pressures (10-12 MPa; *cf.* Figure 6a, b).

Taking all the above into consideration, it is evident that the assumption adopted regarding ground desaturation as well as the anisotropy, have a pronounced effect on the time-development of consolidation and ground convergences and are thus relevant for the shield jamming hazard, which is examined in the next section.

7 ESTIMATION OF THE NECESSARY OVERCUT

Figure 7 shows the longitudinal convergence profile at the crown and sidewalls during TBM advance and after a 1-year-long standstill, for the cases without and with ground desaturation. In the case without desaturation (Figure 7a) the stabilising effect of negative pore pressures (*cf.* Section 3) limits the convergences during TBM advance. After 1 year of standstill, convergences increase due to the consolidation taking place (*cf.* Section 6), but the installed stiff lining provides support to the ground and hence the increase is pronounced only over the unsupported span around the shield. Convergences are at both time instances larger at the sidewalls, where a maximum value of about 20 mm is observed close to the shield tail after a 1-year long standstill.

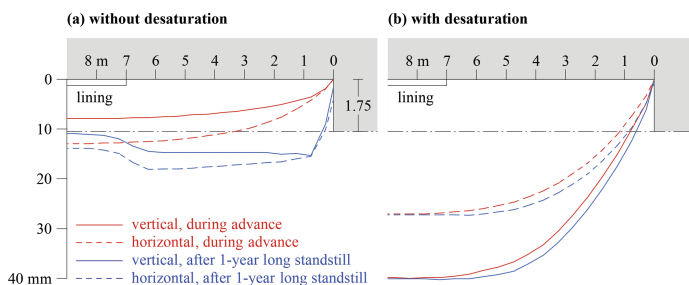


Figure 7. Longitudinal convergence profile, (a), without and, (b), with desaturation.

Desaturation (Figure 7b) eliminates the stabilising effect of suction and thus results in greater convergences (about 3 times greater than in the case without desaturation; compare red lines in Figure 7a, b). The increase in convergence after 1 year of standstill is negligible, since practically no consolidation takes place (*cf.* Section 6). As opposed to the case without desaturation, convergences are larger in both instances at the crown (*cf.* Figure 7a, b), where a maximum value of *ca.* 40 mm is observed at the shield tail, both during advance and after 1 year of standstill.

The plausibility of the numerical results for the case without desaturation can be assessed based upon the GRCs commented in Section 4, which have been computed making the same assumption. There is good agreement with the GRCs for residual matrix parameters, which – considering

that 30-50% of the displacement occurs ahead of the tunnel face – indicate a convergence of 13 - 18 mm for an unsupported tunnel (*cf.* Figures 3, 7a). (The GRC predictions with residual bedding parameters are overly conservative, since bedding strength in the actual 3D problem is only relevant over a small part of the tunnel cross-section). The differences are otherwise attributed to the assumptions embedded in GRCs calculations, particularly those of minimum stiffness over the entire cross-section, isotropic material, and isotropic initial stress state (*cf.* Section 4).

Evidently, the case with desaturation is the most critical for estimating the necessary overcut. The latter is about 40 mm, which is well within the technically feasible range (up to 150 mm). The TBM shield jamming hazard is therefore conclusively not critical for HLW drift construction.

8 CONCLUSIONS

This paper presented a detailed numerical assessment of the TBM shield jamming hazard during the construction of HLW drifts in Opalinus clay, concluding that it is not critical despite the expected squeezing conditions, and contact between shield and ground can be avoided with a moderate overcut of 40 mm. The presented investigations demonstrate the pronounced influence of ground desaturation and material anisotropy on the excess pore pressure dissipation and ground consolidation, and offer practical guidance for considering such aspects in analogous situations. The present work forms the preliminary basis for a much more detailed assessment of shield jamming and lining overstressing over the HLW drift life-cycle, which will also consider different options for the lining system and propose sustainable and robust design solutions.

REFERENCES

- Anagnostou, G. 2009. The effect of advance-drainage on the short-term behaviour of squeezing rocks in tunneling. In *Proceedings of the 1st International Symposium on Computational Geomechanics* (pp. 668–679). International Center of Computational Engineering.
- Armand, G., Conil, N., Talandier, J. & Seyedi, D.M. 2017. Fundamental aspects of the hydromechanical behaviour of Callovo-Oxfordian claystone: from experimental studies to model calibration and validation. *Computers and Geotechnics* 85: 277–286.
- Brauchart, A., Nordas, A. & Anagnostou, G. 2021. Calibration of the Anisotropic Linearly Elastic, Perfectly Plastic Model (ALEPP) based upon Bülach and Mont Terri Triaxial Test Results (rev. B). ETH Zurich, Zurich (unpublished preliminary draft).
- Chenevert, M.E. 1969. Adsorptive pore pressures of argillaceous rocks. In *The 11th US Symposium on Rock Mechanics*: 599–627.
- Crisci, E., Laloui, L., & Giger, S. 2021. TBO Bülach-1-1: Data Report. Dossier IX: Rock-mechanical and Geomechanical Laboratory Testing. Nagra Arbeitsbericht NAB 20-08.
- Crisci, E., Laloui, L., & Giger, S. 2022. TBO Trüllikon-1-1: Data Report. Dossier IX: Rock-mechanical and Geomechanical Laboratory Testing. Nagra Arbeitsbericht NAB 20-09.
- Crisci, E., Laloui, L., & Giger, S. 2022. TBO Bözberg-2-1: Data Report. Dossier IX: Rock-mechanical and Geomechanical Laboratory Testing. Nagra Arbeitsbericht NAB 21-22.
- Dassault Systèmes 2019. ABAQUS 2019 Theory manual. Dassault Systèmes Simulia Corp., Providence, Rhode Island.
- Mazurek, M., Hurford, A.J. & Leu, W. 2006. Unravelling the multi-stage burial history of the Swiss Molasse Basin: integration of apatite fission track, vitrinite reflectance and biomarker isomerisation analysis. *Basin Research* 18(1): 27–50.
- Morosoli, D., Cantieni, L., Anagnostou, G. 2023. Design considerations for deep caverns in Opalinus Clay. *World Tunnel Congress "Expanding underground - Knowledge & Passion to Make a Positive Impact on the World"*, Athens.
- Nagra 2016. ENSI-Nachforderung zum Indikator "Tiefenlage im Hinblick auf bautechnische Machbarkeit" in SGT Etappe 2. Geomechanische Unterlagen. Nagra Arbeitsbericht NAB 16–43.
- Nordas, A.N. & Anagnostou, G. 2021. Analytical short-term ground response curves for a linearly elastic, brittle-plastic constitutive model, Rev. A. ETH Zurich, 20.06.21.
- Ramoni, M. & Anagnostou, G. 2010. Tunnel boring machines under squeezing conditions. *Tunnelling and Underground Space Technology* 25(2): 139–157.
- Vrakas, A., Dong, W. & Anagnostou, G. 2018. Elastic deformation modulus for estimating convergence when tunnelling through squeezing ground. *Géotechnique* 68(8): 713–728.